Rapid decay of Martian Global Dust Storms driven by small-scale deposition processes in the lower planetary boundary layer.

Lulu Li, Cong Sun, Siteng Fan, *Department of Earth and Space Sciences, Southern University of Science and Technology, Shenzhen, China*, **Chun Zhao, Yongxuan Zhao, Tao Li,** *CAS Key Laboratory of Geospace Environment, School of Earth and Space Sciences, University of Science and Technology of China, Hefei, China*, **Claire E. Newman,** *Aeolis Research, Chandler, Arizona, U.S.A*.

Introduction

Atmospheric dust is a key driver of Martian climate and weather, analogous to the role of water vapor on Earth [12]. Through its interaction with solar and infrared radiation, dust modulates atmospheric heating, circulation, and seasonal variability [3] [4]. A crucial component of the Martian dust cycle is dry deposition, which regulates the vertical and horizontal distribution of airborne dust and ultimately determines its atmospheric residence time[5] [6].

While gravitational sedimentation is the primary process considered in most Martian general circulation models (GCMs), several additional near-surface mechanisms–such as turbulent transfer, Brownian diffusion, impaction, interception, and rebound–are known from terrestrial wind tunnel experiments to significantly influence aerosol removal [13][14]. These processes have been incorporated into Earth-based atmospheric models using resistance-based approaches, yet remain largely unaccounted for in Mars GCMs [5] [6]. Furthermore, the lack of particle-size resolution in most Martian models limits their ability to capture important microphysical feedbacks [2] [7] [10], particularly under dust-rich conditions such as global dust storms (GDSs).

In this study, we implement a new, physically based, size-resolved dry deposition scheme into the MarsWRF general circulation model. The scheme includes a comprehensive set of near-surface deposition processes and explicitly resolves eight discrete dust particle size bins. Our objective is to evaluate how this improved representation of dry deposition affects the Martian dust cycle during non-global dust storm (non-GDS) years, and to investigate the role of particle-size-dependent removal in shaping the evolution and decay of global dust storms.

Methodology

The dry deposition scheme presented in this study is based on [13], which was specifically developed for rough surfaces. This scheme encompasses all types of dry deposition processes (as illustrated in Figure 1). A key concept in the study of dry deposition processes is

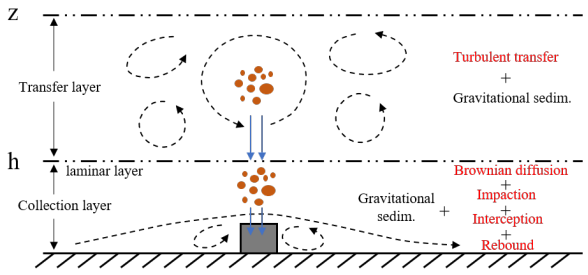

Figure 1: Schematic of the two-layer model for dry deposition. Adapted from [13] and [15].

the deposition velocity, described as follows:

$$v_d(z) = \left(r_g + \frac{r_s - r_g}{\exp\left(\frac{r_a}{r_g}\right)} \right)^{-1},$$

where z is the height above the surface (m), r_g is the gravitational resistance, r_a is the aerodynamic resistance, and r_s is the surface collection resistance.

The gravitational resistance r_g is defined as the inverse of particle gravitational sedimentation velocity (v_g, $m\ s^{-1}$), i.e.,

$$r_g = v_g^{-1}.$$

For the aerodynamic resistance r_a, it focuses on the effects of turbulent transfer occurring in the transfer layer as shown in Figure 1. The formula is given by

$$r_a(z) = \frac{\mathrm{Sc}_T}{\kappa u_*} \left[\ln\left(\frac{z - z_d}{h_c - z_d} \right) - \psi_m \right].$$

where κ is the von Karman constant, $_m$ is the stability function, z_d is the zero-plane displacement height, h_c is the height of a roughness element. In this work, sand particles are assumed to be the roughness elements on the surface with h_c being 0.1 mm.

The surface collection resistance, r_s, is governed by a combination of near-surface microphysical processes, including Brownian diffusion, impaction, interception, rebound, and gravitational sedimentation. It is expressed as:

$$r_s = \left\{ R \cdot v_{dm} \left[\frac{E}{C_d} \cdot \frac{\tau_c}{\tau} + E_s^B + E_s^{im} \right] + v_g \right\}^{-1},$$

where R denotes the fraction of particles that remain adhered to the rough surface after accounting for rebound, v_{dm} is the conductance for momentum transfer, C_d represents the drag coefficient for the isolated roughness element. The term E represents the combined collection efficiency due to Brownian diffusion, impaction, and interception on the side areas of surface roughness elements. E_s^B and E_s^{im} denote the collection efficiencies due to Brownian diffusion and impaction, respectively, on the upward-facing surface.

Results

To account for the strong size dependence of dry deposition velocity, eight particle size bins ranging from approximately 0.039 μm to 10 μm are used to represent the lifted dust particle size distribution. In the Exp-Microphy experiment, a size-resolved dry deposition scheme is implemented at the lowest model level (eta = 0.998), while the Exp-Gravity experiment includes only gravitational sedimentation as the dust removal mechanism. Above the near-surface layer, both experiments apply gravitational sedimentation uniformly to all particle sizes.

Figure 2 illustrates the spatial distribution of the difference in near-surface dry deposition velocity between Exp-Microphy and Exp-Gravity across the eight particle size bins during the non-GDS year. The inclusion of the full dry deposition scheme leads to consistently higher deposition velocities for all sizes. The enhancement exhibits a clear seasonal pattern, with the largest differences occurring during southern spring and summer, and smaller differences during the northern warm seasons. The magnitude of the enhancement increases with particle size up to the 0.884 μm bin–reaching a peak difference of over 0.024 m/s–then declines for larger particles.

Spatial variations further reveal size-dependent patterns. For smaller particles, the most significant enhancements are concentrated in the southern mid-latitudes (around $30^\circ S$), especially along the retreating edge of the CO_2 seasonal ice cap, coinciding with regions of elevated friction velocity. In contrast, for larger particles, the greatest enhancements shift toward the high latitudes of the northern hemisphere, highlighting the size- and latitude-dependent nature of the additional dry deposition processes.

Figure 3 compares observational records of global dust storms (GDSs) with model simulations. Observations (Figure 3a) show that GDSs occurred in Mars Years (MY) 25, 28, and 34, with a consistent seasonal preference for southern spring and summer [1] [8] [9]. The events in MY25 and MY34 initiated near $L_s = 185^\circ$, rapidly expanded to global scales, and reached peak mid-level atmospheric temperatures (T15) of ∼216 K and ∼214 K, respectively. In contrast, the MY28 storm

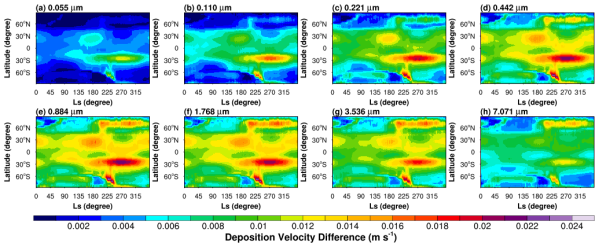

Figure 2: Seasonal variation of the difference of total dry deposition velocity in Exp-Microphy to gravitational sedimentation velocity in Exp-Gravity corresponding to the 8 bins of dust particles.

began later, around $L_s = 260^\circ$, and was weaker,with T15 peaking near 210 K. All three events underwent rapid decay following peak intensity, with dissipation completed by early southern summer. The strongest storm (MY25) persisted the longest, while the weaker MY28 event decayed more quickly.

Simulated results in Figures 3b and 3c show that both Exp-Gravity and Exp-Microphy successfully capture the key seasonal characteristics of GDSs, including their timing (between $L_s = 185^\circ$ and $L_s = 300^\circ$) and intensity (T15 > 210 K). In Exp-Gravity, GDSs occur in years 4, 7, and 11, with peak T15 reaching ∼220 K. Exp-Microphy simulates similarly intense storms in years 12, 18, and 19, though with a delayed onset.

While both experiments slightly overestimate GDSs strength, Exp-Microphy uniquely captures the rapid decay phase, a long-standing challenge in Martian dust modeling. In Exp-Gravity, storm decay is gradual, beginning around $L_s = 325^\circ$ and extending well into the following year. In contrast, Exp-Microphy shows much faster dissipation, with dust loading and T15 returning to background levels by early northern spring. This shortens the decay period by over half a Martian year and brings the seasonal temperature evolution into much better agreement with observations–particularly the cooler conditions during northern spring and summer, attributed to reduced atmospheric dust loading [2] [7].

Summary

The implementation of a size-resolved dry deposition scheme in the lower part of the planetary boundary layer in MarsWRF enhances the model's ability to (1) accurately represent near-surface dust removal across a wide particle size range, (2) effectively remove small particles through additional deposition processes, and (3) realistically capture the decay phase of global dust storms–particularly the timing and magnitude of post-storm atmospheric cooling.

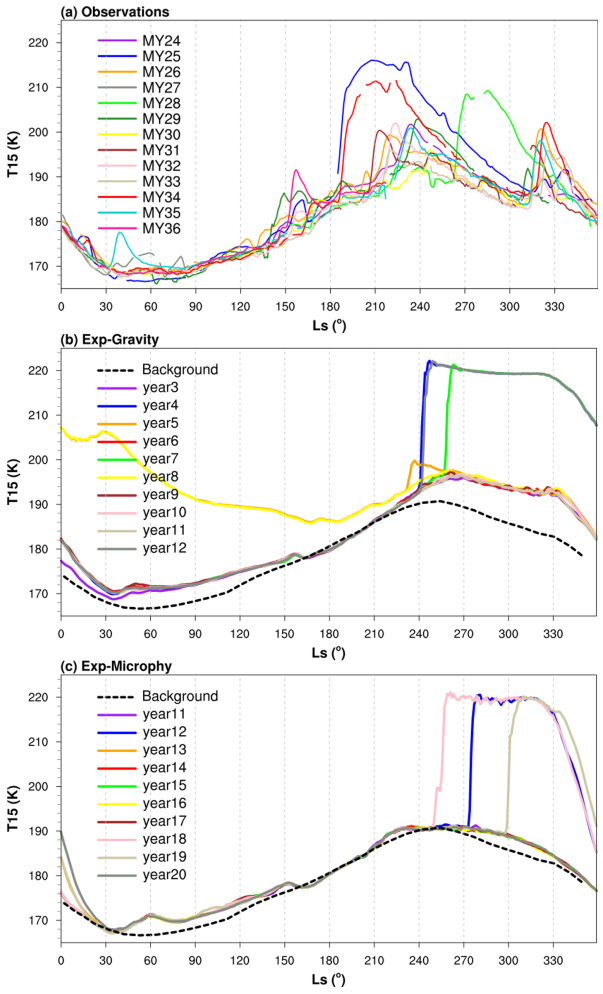

Figure 3: Seasonal variation in zonal-, latitudinal- and daily-mean T15 ($42.5°S$ to $42.5°N$) for (a) multi-years observations. The Mars Analysis Correction Data Assimilation (MACDA) dataset version 1.0 is used for MY 24 to 27, and Mars Climate Sounder (MCS) observations for MY 28 to 34. These MACDA and MCS temperatures are corrected using a vertical weighting function centered at 25 km, similar to the Viking IRTM 15-µm channel[11]. Panels (b) and (c) show the same as (a), but for the MarsWRF simulated T15 for Exp-Gravity and Exp-Microphy over ten years, respectively. The black dashed line denotes the climatological background, with storm peaks removed from the averaged T15, as provided by [2].

References

[1] Bruce A. Cantor. "MOC observations of the 2001 Mars planet-encircling dust storm". In: *Icarus* 186.1 (Jan. 2007), pp. 60–96. ISSN: 00191035. DOI: 10.1016/j.icarus.2006.08.019.

[2] C. Gebhardt et al. "Fully interactive and refined resolution dimulations of the Martian dust cycle by the MarsWRF model". In: *Journal of Geophysical Research: Planets* 125.9 (Sept. 2020), e2019JE006253. ISSN: 2169-9097, 2169-9100. DOI: 10.1029/2019JE006253.

[3] Peter Gierasch and Richard Goody. "A study of the thermal and dynamical structure of the martian lower atmosphere". In: *Planetary and Space Science* 16.5 (May 1968), pp. 615–646. ISSN: 00320633. DOI: 10.1016/0032-0633(68)90102-5.

[4] Robert M. Haberle, Conway B. Leovy, and James B. Pollack. "Some effects of global dust storms on the atmospheric circulation of Mars". In: *Icarus* 50.2 (May 1982), pp. 322–367. ISSN: 00191035. DOI: 10.1016/0019-1035(82)90129-4.

[5] Melinda A. Kahre et al. "The Mars dust cycle". In: *The Atmosphere and Climate of Mars*. Ed. by Robert M. Haberle et al. 1st ed. Cambridge University Press, June 2017, pp. 295–337. ISBN: 978-1-139-06017-2 978-1-107-01618-7. DOI: 10.1017/9781139060172.010.

[6] James R. Murphy et al. "Numerical simulations of the decay of Martian global dust storms". In: *Journal of Geophysical Research: Solid Earth* 95 (B9 1990), pp. 14629–14648. ISSN: 2156-2202. DOI: 10.1029/JB095iB09p14629.

[7] Claire E. Newman and Mark I. Richardson. "The impact of surface dust source exhaustion on the martian dust cycle, dust storms and interannual variability, as simulated by the MarsWRF General Circulation Model". In: *Icarus* 257 (Sept. 2015), pp. 47–87. ISSN: 0019-1035. DOI: 10.1016/j.icarus.2015.03.030.

[8] A. Sánchez-Lavega et al. "The onset and growth of the 2018 Martian global dust storm". In: *Geophysical Research Letters* 46.11 (2019), pp. 6101–6108. ISSN: 1944-8007. DOI: 10.1029/2019GL083207.

[9] Michael D. Smith. "THEMIS observations of the 2018 Mars global dust storm". In: *Journal of Geophysical Research: Planets* 124.11 (Nov. 2019), pp. 2929–2944. ISSN: 2169-9097, 2169-9100. DOI: 10.1029/2019JE006107.

[10] Yemeng Wang et al. "Effect of dust particle size on the climate of Mars". In: *Planetary and Space Science* 208 (Nov. 2021), p. 105346. ISSN: 00320633. DOI: 10.1016/j.pss.2021.105346.

[11] R Wilson. “The Martian atmosphere during the Viking mission, I Infrared measurements of atmospheric temperatures revisited”. In: *Icarus* 145.2 (June 2000), pp. 555–579. ISSN: 00191035. DOI: 10.1006/icar.2000.6378.

[12] Zhaopeng Wu et al. “Earth-like thermal and dynamical coupling processes in the Martian climate system”. In: *Earth-Science Reviews* 229 (June 2022), p. 104023. ISSN: 00128252. DOI: 10.1016/j.earscirev.2022.104023.

[13] J. Zhang and Y. Shao. “A new parameterization of particle dry deposition over rough surfaces”. In: *Atmospheric Chemistry and Physics* 14.22 (2014), pp. 12429–12440. DOI: 10.5194/acp-14-12429-2014.

[14] L Zhang. “A size-segregated particle dry deposition scheme for an atmospheric aerosol module”. In: *Atmospheric Environment* 35.3 (2001), pp. 549–560. ISSN: 13522310. DOI: 10.1016/S1352-2310(00)00326-5.

[15] Xiao-Xiao Zhang et al. “Parameterization schemes on dust deposition in northwest China: Model validation and implications for the global dust cycle”. In: *Atmospheric Environment* 209 (July 2019), pp. 1–13. ISSN: 13522310. DOI: 10.1016/j.atmosenv.2019.04.017.